Theoretical Study on Single-Scattering Properties of Ice Particles of Different Orientation at 94 GHz

Jin-Hu Wang[1, 2, *], Jun-Xiang Ge[1, 2], and Ming Wei[1, 2]

Abstract—The single-scattering properties of hexagonal columns and plates were studied using Discrete Dipole Approximation at 94 GHz, including scattering efficiency, absorption efficiency, asymmetry factor, backscattering cross section and phase function. Random and horizontal orientations of particles were compared, and 35 sizes of maximum dimension D ranging from 1 μm to 10 mm were selected. The results indicate that scattering and absorption efficiencies of horizontally oriented hexagonal columns are larger than those of the randomly oriented ones, whereas this phenomenon does not appear to hexagonal plates. The asymmetry factor of horizontally oriented hexagonal plates has a negative value, which means that the backscattered energy is more than forward energy when the particle is large enough. The backscattering cross sections of horizontally oriented hexagonal columns and plates are larger than those of random orientation, which can be explained by that different cross sections of particles will be exposed to incident plane wave. When the particle size is smaller than incident wavelength, little scattering energy difference between random and horizontal orientation exists, while if the particle is larger than incident wavelength, a turning point will happen at $\theta = 110°$, which can be explained by the theory of energy conservation.

1. INTRODUCTION

Cirrus clouds are mainly composed of ice crystals located in the upper troposphere and play an important role in the climate system of the earth [1]. To understand the impact of clouds on climate systems, many researchers have calculated the single-scattering properties of ice crystals by solving the basic electromagnetic wave equations. Due to the irregularity of cirrus cloud ice crystals, numerical methods have been developed such as T-matrix [2], Finite Difference Time Domain(FDTD) [3], Improved Geometric Optic Method(IGOM) [4], and Discrete Dipole Approximation(DDA) [5]. Yang et al. [6] in 2005 computed single-scattering properties of ice particles from near far infrared spectral regions using a composite method based on a combination of FDTD, T-method, IGOM, and Lorenz-Mie. In 2007, Hong [7] studied millimeter wavelength radar backscattering properties at 94 GHz using DDA method and Lorenz-Mie theory. Few works, however, have discussed the single-scattering properties of ice particles based on selection of orientations. Zhang [8] has pointed out the difference of backscattering cross sections between ice crystals with 2D orientations and 3D orientations. Results show that the orientation effects using vertical oriented 94 GHz radar cannot be ignored. This raises a question: how can the difference in single-scattering properties of ice particles at 94 GHz be explained by their different orientations? The objective of this paper is to study the difference in single-scattering properties by considering scattering efficiency, absorption efficiency, asymmetry factor, backscattering cross section, and phase function between randomly and horizontally oriented hexagonal columns and plates using the DDA method.

2. DISCRETE DIPOLE APPROXIMATION METHOD

The discrete dipole approximation (DDA) is a general method; it can compute single-scattering properties of arbitrary target. Initially DDA was proposed by Purcell and Pennypacker [9], who replaced the scatter by a set of point dipoles. Draine and Flatau [10] developed the DDA model and provided relevant codes. The principle advantage of DDA is that it is flexible as regards the geometry of the target. One limitation, however, is that the interdipole spacing must be sufficiently small compared to the wavelength in order to obtain the desired accuracy, which requires both large computer memory and long computation time for larger particles [11].

The basic principle of DDA is as follows [11].

Assuming that the polarizability is α_j and that the dipole moment is $\overrightarrow{P_j}$ for the jth dipole, the DDA model attempts to find the solution for a self-consistent set of dipole moments, which can be described in the following formula:

$$\overrightarrow{P_j} = \alpha_j \vec{E}_{ext,j} = \alpha_j \left(\vec{E}_{inc,j} - \sum_{k \neq j} A_{jk} \overrightarrow{P_k} \right) \tag{1}$$

where $\vec{E}_{inc,j}$ is the electric field at the position j due to the incident plane wave, and $-A_{jk}\overrightarrow{P_k}$ is the contribution to the electric field at the position j due to the dipole at position k. A_{jk} can be expressed by a function of angular wave-number K and the relative position of dipoles j and k. The mathematical expression of A_{jk} can be found in relevant literature [5]:

$$A_{jk} = \frac{\exp(ikr_{jk})}{r_{jk}} \left[k^2(\hat{r}_{jk}\hat{r}_{jk} - \bar{\bar{I}}_3) + \frac{ikr_{jk} - 1}{r_{jk}^2} \left(3\hat{r}_{jk}\hat{r}_{jk} - \bar{\bar{I}}_3 \right) \right] \tag{2}$$

where $k = \omega/c$, $r_{jk} = |\vec{r}_j - \vec{r}_k|$, $\hat{r}_{jk} = (\vec{r}_j - \vec{r}_k)/r_{jk}$, $\bar{\bar{I}}_3$ is the 3×3 identity matrix.

$$\text{When} \quad j = k, \text{ then } A_{jj} = \alpha_j^{-1} \tag{3}$$

Multiplied by α_j^{-1}, Eq. (1) can be rewritten as

$$\overrightarrow{P_j} \cdot \alpha_j^{-1} = \vec{E}_{inc,j} - \sum_{k \neq j} A_{jk} \overrightarrow{P_k} \tag{4}$$

When substituting (3) into (4), we can get the following equation:

$$\sum_{k=1}^{N} A_{jk} \overrightarrow{P_k} = \vec{E}_{inc,j} \tag{5}$$

where N is the total number of dipoles. Once (5) has been solved for the unknown polarizations $\overrightarrow{P_j}$, the single-scattering parameters including the scattering and absorption efficiencies, the asymmetry parameter and the phase matrix of scattering may be evaluated.

The DDSCAT is a software package, which can calculate scattering properties of electromagnetic waves by targets with arbitrary geometries using DDA theory and is written in Fortran 90 [10]. This software includes some predetermined shapes such as spheres, ellipsoids, finite cylinder, finite hexagonal prism, tetrahedron, multilayer rectangular slab, triangular prism and others.

Figure 1 shows the general process of computing the single-scattering properties of studied target. Once the codes of ddscat.par file are correctly set according to actual demand, the single-scattering properties of target can be obtained after clicking ddscat.exe.

Although DDA can describe any geometry, it is limited by a minimum distance d that should exist between dipoles. In order to accurately compute the scattering properties of targets, the following criterion must be satisfied

$$|m|\,kd < 0.5 \tag{6}$$

where m is the complex refractive index of target material and k the wave-number of the surrounding medium.
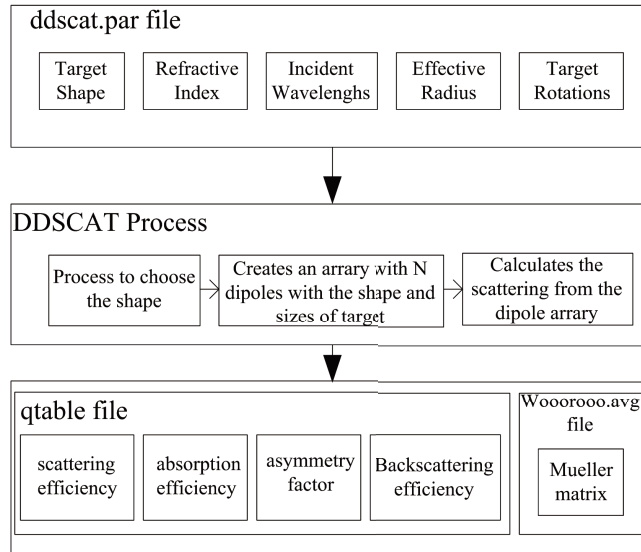
Figure 1. General process of computing scattering efficiency, absorption efficiency, asymmetry factor, backscattering cross section and phase function of target.

It must be emphasized that DDA is not suitable for very large values of the size parameter or very large values of the refractive index because of CPU speed and computer memory currently available on scientific workstations [10].

3. SINGLE-SCATTERING PROPERTIES OF HEXAGONAL COLUMNS AND PLATES

Cirrus clouds are composed of ice particles of various sizes and shapes, although hexagonal plates and columns are the most often encountered [8]. Sizes of ice crystals can range from $< 10\,\mu\text{m}$ to many thousands of microns [12]. Figures 2(a) and (b) show the geometry of hexagonal columns and hexagonal plates, respectively.

The empirical relationship between side length a and length L is summarized by Hong [13]:

$$\text{Hexagonal column:} \begin{cases} a = 0.35L & (L < 100\,\mu\text{m}) \\ a = 3.48L^{0.5} & (L \geq 100\,\mu\text{m}) \end{cases} \tag{7}$$

$$\text{Hexagonal plate:} \begin{cases} L = 2a & (a \leq 2\,\mu\text{m}) \\ L = 2 + \dfrac{2.4883a^{0.474} - 2}{4}(a - 1) & (2\,\mu\text{m} < a < 5\,\mu\text{m}) \\ L = 2.4883a^{0.474} & (a \geq 5\,\mu\text{m}) \end{cases} \tag{8}$$
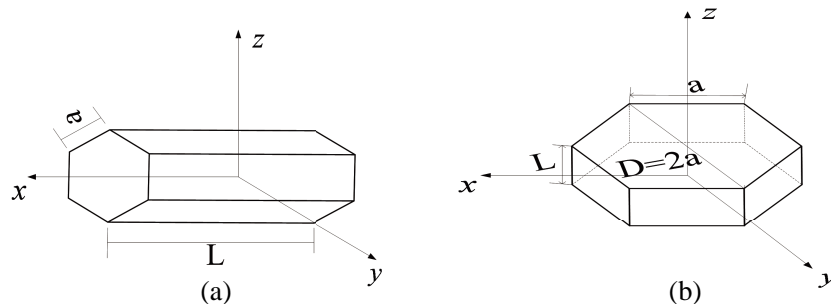

Figure 2. The geometry for (a) hexagonal column and (b) hexagonal plate.

The existence of horizontally oriented ice crystals has been confirmed by several lidar observations. Polarization and directionality of the Earth's Reflectance (POLDER) instruments have shown that approximately 40% of the ice crystals in cirrus clouds are horizontally oriented [14, 15]. The scattering properties of randomly oriented ice crystals studied by some scholars [4, 7, 13, 16], however, are also very significant. Based on this fact, we define two orientation models: a random orientation model and a horizontal orientation model. The random orientation model will be referred to as "3D orientation" where particles described can freely rotate about xyz axes; the second model is the horizontal orientation model, which will be referred to as "2D orientation". To "2D orientation", the major dimension or long rotationally asymmetric axis of described particles is on a horizontal plane; the broad hexagonal face of the plate is on a horizontal plane, and the plate can freely rotate about the z axis, while the long symmetric axis of a column on a horizontal plane can freely rotate about the x and z axes. In order to model randomly oriented symmetrical ice particles of hexagonal columns and plates in space, we average the scattering properties over 1000 orientations. For horizontally oriented ice particles, we average the scattering properties over about 100 orientations for hexagonal columns and 10 for hexagonal plates.

In this paper, the incident electromagnetic wave propagates along the z axis and is linearly polarized. The range of particle size considered in this paper is from $1\,\mu$m to $10\,$mm in terms of the maximum dimension D which equals L of the hexagonal columns and equals $2a$ of the hexagonal plates. 35 sizes of D are computed. The refractive index for the ice crystal is assumed $m_{ice} = 1.782 + 0.00270i$ [17] at $94\,$GHz and the density of ice used is $0.917\,$gcm^{-3} [7].
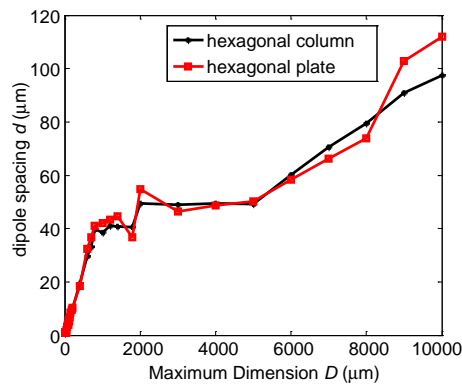

Figure 3. Dipole spacing d used for the DDA calculation as a function of maximum dimension D for hexagonal columns and plates.
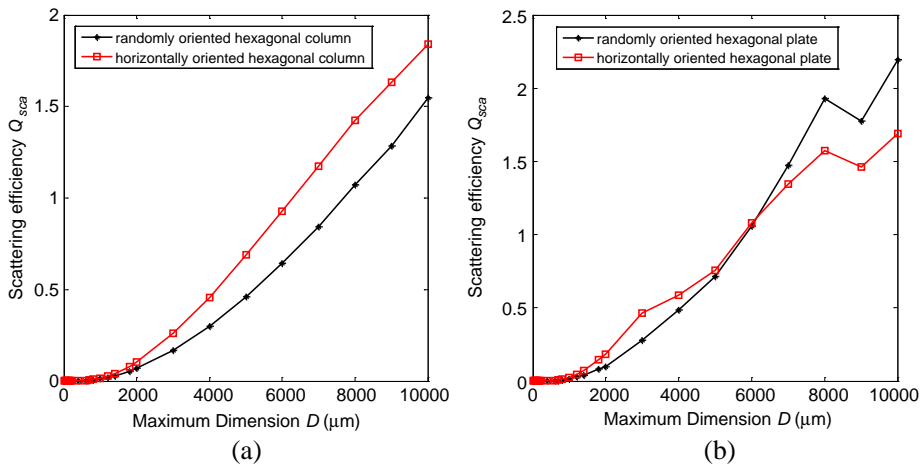

Figure 4. Variations in scattering efficiency Q_{sca} as a function of maximum dimension D for hexagonal column and hexagonal plate of random and horizontal orientation at $94\,$GHz.
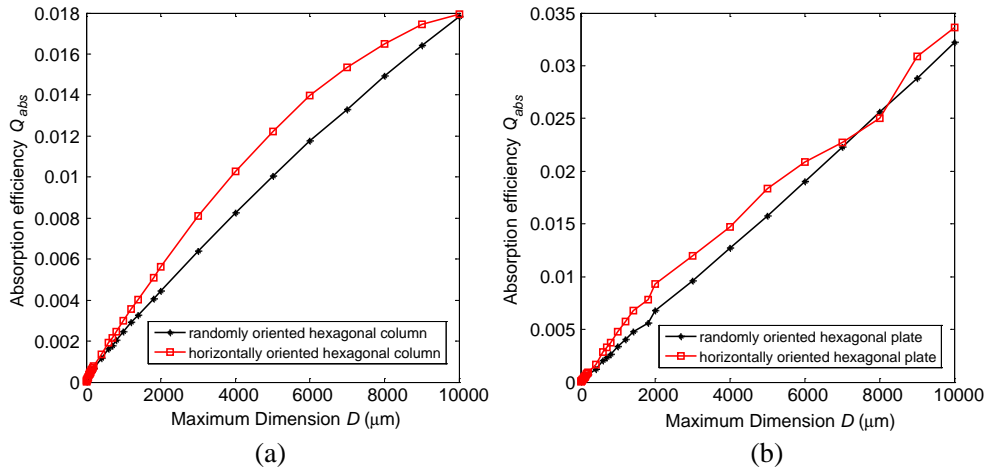
Figure 5. Variations in absorption efficiency Q_{abs} as a function of maximum dimension D for hexagonal column and hexagonal plate of random and horizontal orientation at 94 GHz.
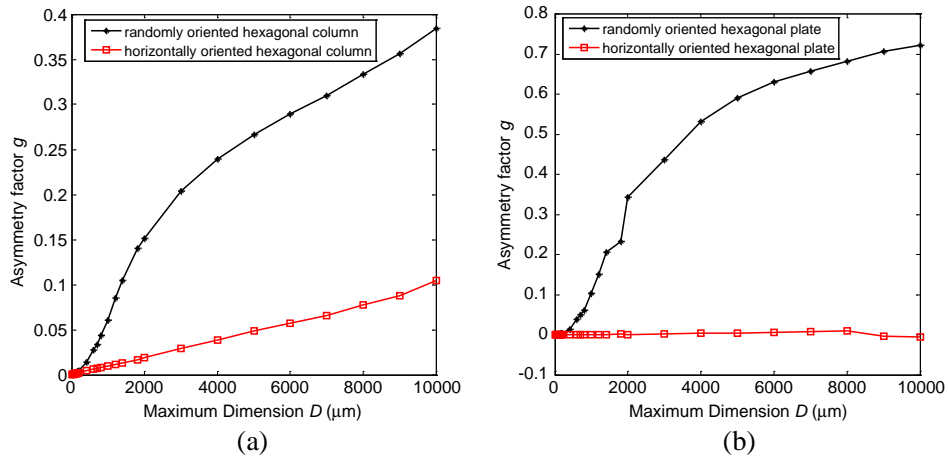

Figure 6. Variations in asymmetry factor g as a function of maximum dimension D for hexagonal columns and hexagonal plates of random and horizontal orientation at 94 GHz.
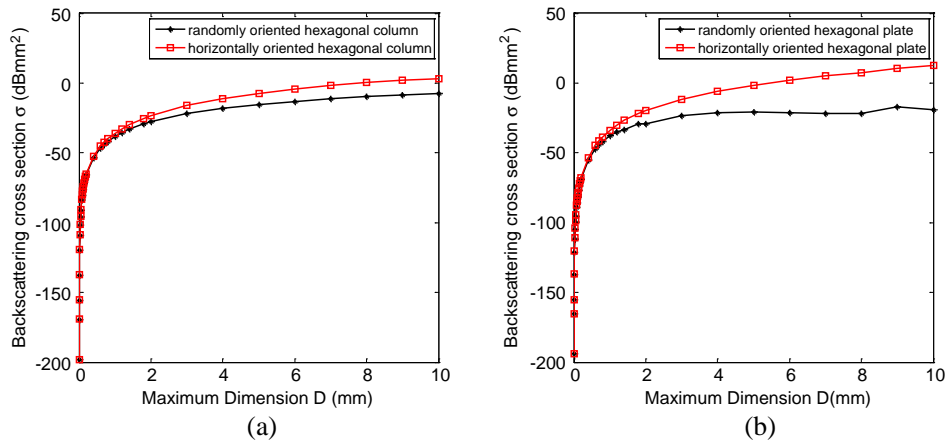

Figure 7. Variations in backscattering cross section σ as a function of maximum dimension D for hexagonal column and hexagonal plate of random and horizontal orientation at 94 GHz.

Figure 3 shows the ice crystal dipole spacing d of hexagonal columns and plates used for the DDA computation as a function of the maximum dimension D (hexagonal column: $D = L$; hexagonal plate: $D = 2a$).

Figures 4, 5, 6, 7 show scattering efficiency Q_{sca}, absorption efficiency Q_{abs}, asymmetry factor g and backscattering cross section σ as functions of maximum dimension D at 94 GHz for hexagonal columns and plates of random and horizontal orientation, respectively.

It is found that scattering efficiency and absorption efficiency of horizontally oriented hexagonal columns are larger than that of random orientation. On the other hand, scattering efficiency and absorption efficiency of hexagonal plates do not exhibit this phenomenon because of weak oscillation, which is illustrated in Figures 4 and 5. Additionally, scattering and absorption efficiencies of hexagonal columns and plates generally increase with the growth of D, regardless of "3D orientation" or "2D orientation". For large particles, absorption efficiency is smaller than scattering efficiency because imaginary part value of ice refractive index is very small ($\varepsilon_i \approx 0.00270$), and it determines the absorption efficiency, whereas for small particles, absorption efficiency dominates. This result agrees with that in [18].

Asymmetry factor g, which is the first-order moment of the phase function, is positive if the particle
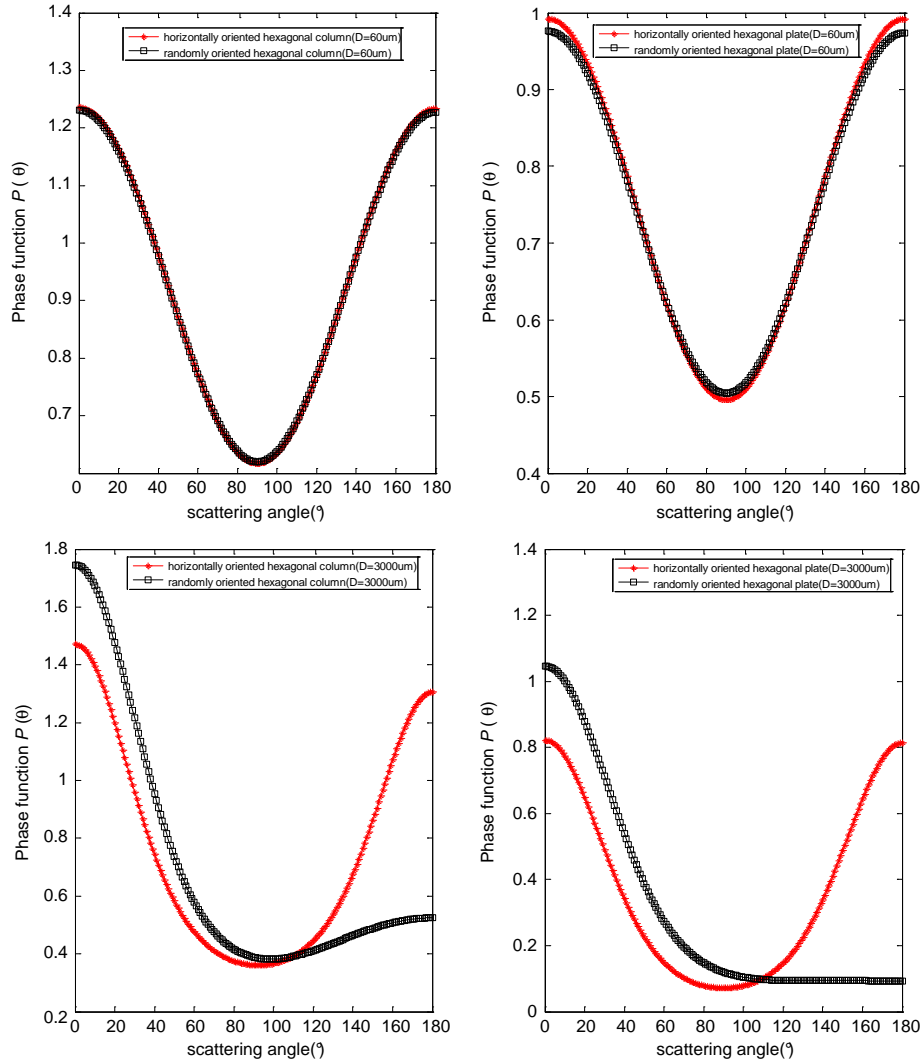

Figure 8. Phase function $P(\theta)$ for hexagonal columns and plates of random and horizontal orientation at 94 GHz with maximum dimensions D of 60 μm and 3000 μm.

scatters more electromagnetic waves in a forward direction. g is negative if backscattering energy is more than forward scattering energy. When the backscattering energy is equal to forward scattering energy, g is equal to zero. Figure 6 shows that the asymmetry factor of horizontally oriented hexagonal columns and plates is smaller than that of random orientation. We also find that the forward scattering energy is nearly equal to the backward scattering energy when the particle is small. The growth rate of the forward scattering energy of random orientation is faster than those of horizontal orientation. In addition, g of the horizontally oriented hexagonal plate has a negative value, which means that the backscattering energy is more than forward scattering energy when particle exceeds $8000\,\mu\mathrm{m}$.

In fact, the orientation of ice crystals relative to the incidence plane wave has significant impact on the backscattering cross sections. Figure 7 shows the backscattering cross section of horizontally oriented hexagonal columns and plates is larger than that of random orientation because "2D oriented particles" always have larger cross section than "3D orientated particles" when particles are exposed to incident plane electromagnetic wave.

The angular distribution of the scattering energy is illustrated by phase function $P(\theta)$. "V-pattern" variation of phase function versus scattering angle is illustrated when the maximum dimension $D = 60\,\mu\mathrm{m}$ in Figure 8. Little scattering energy difference between random and horizontal orientation exists in this case. When the maximum dimension $D = 3000\,\mu\mathrm{m}$, the scattering energy of randomly oriented hexagonal columns and plates is larger than that of horizontal orientation at $0 \leq \theta \leq 110°$, and it will be inversed at $110° \leq \theta \leq 180°$.

4. CONCLUSION

Millimeter-wavelength radar has emerged as an important tool in characterizing scattering properties of cirrus clouds. This paper studies the single-scattering properties of hexagonal columns and plates with random and horizontal orientations using DDA.

The results show that: (1) Scattering and absorption efficiencies of hexagonal columns and plates generally increase with the growth of D regardless of "3D orientation" or "2D orientation", and these values at "2D orientation" are larger than those at "3D orientation". Absorption efficiency of particles is much smaller than scattering efficiency due to the small imaginary part value of ice refractive index for large particles. (2) Asymmetry factor of hexagonal columns and plates at "2D orientation" is smaller than the case of "3D orientation". Moreover, the asymmetry factor of hexagonal plates at "2D orientation" has negative values, which means that the backscattered energy is more than forward energy in this case. (3) The backscattering cross section of hexagonal columns and plates at "2D orientation" is larger than those at "3D orientation" because "2D orientation" particles always have larger cross section than "3D orientation" particles. (4) When the particle is small enough relative to incident wavelength, there is almost no difference of scattering energy between "2D orientation" and "3D orientation". The scattering energy of hexagonal columns and plates at "3D orientation" is larger than that of "2D orientation" at $0 \leq \theta \leq 110°$ when particles are large enough, and it will be inversed at $110° \leq \theta \leq 180°$.

ACKNOWLEDGMENT

REFERENCES

1. Liou, K. N., "Influence of cirrus clouds on weather and climate processes: A global perspective," *Mon. Wea. Rev.*, Vol. 14, 1167–1199, 1986.

2. Mishchenko, M. I., L. D. Travis, and D. W. Mackowski, "T-matrix computations of light scattering by nonspherical particles: A review," *J. Quant. Spectrosc. Radiant. Transfer*, Vol. 55, 535–575, 1996.

3. Yang, P. and K. N. Liou, "Finite-difference time domain method for light scattering by small ice crystals in three-dimensional space," *J. Opt. Soc. Am. A*, Vol. 13, 2072–2085, 1996.

4. Yang, P., K. N. Liou, K. Wyser, and D. Mitchell., "Parameterization of the scattering and absorption properties of individual ice crystals," *J. Geophys. Res.*, Vol. 105, 4699–4718, 2000.

5. Draine, B. T. and P. J. Flatau, "Discrete-dipole approximation for scattering calculation," *J. Opt. Soc. Am. A*, Vol. 11, 1491–1499, 1994.

6. Yang, P., H. Wei, H.-L. Huang, B. A. Baum, Y. X. Hu, et al., "Scattering and absorption property database for nonspherical ice particles in the near-through far-infrared spectral region," *Appl. Opt.*, Vol. 44, 5512–5523, 2005.

7. Hong, G., "Radar backscattering properties of nonspherical ice crystals at 94 GHz," *J. Geophys. Res.*, Vol. 112, D22203–D008839, 2007, Doi: 10.1029/2007JD008839.

8. Zhang, Z., "Computation of the scattering properties of nonspherical ice crystals," 57–78, Thesis of Degree of Master of Science, Texas A&M University, 2004.

9. Purcell, E. M. and C. R. Pennypacker, "Scattering and absorption of light by nonspherical dielectric grains," *Astrophys J.*, Vol. 186, 705–714, 1973.

10. Draine, B. T. and P. J. Flatau, "User guide for the discrete dipole approximation code DDSCAT 7.2," *Computational Physics*, 1–95, Princeton University Observatory, 2012.

11. Liu, G., "Approximation of single scattering properties of ice and snow particles for high microwave frequencies," *Journal of the Atmospheric Sciences*, Vol. 61, 2441–2456, 2004.

12. Vogelmann, A. M. and T. P. Ackerman, "Relating cirrus cloud properties to observed fluxes: A critical assessment," *J. Atmos. Sci.*, Vol. 52, 4285–4301, 1995.

13. Hong, G., "Parameterization of scattering and absorption properties of nonspherical ice crystals at microwave frequencies," *J. Geophys. Res.*, Vol. 112, D11208, 2007, Doi: 10.1029/2006JD008364.

14. Sassen, K., "The polarization lidar technique for cloud research: A review and current assessment," *Bull. Am. Meteorol. Soc.*, Vol. 72, 1848–1866, 1991.

15. Noel, V. and H. Chepfer, "Study of ice crystal orientation in cirrus clouds based on satellite polarized radiance measurements," *J. Atmos. Sci.*, Vol. 61, No. 16, 2073–2081, 2004.

16. Takano, Y. and K. N. Liou, "Radiative transfer in Cirrus clouds. Part III, Light scattering by irregular ice crystals," *Journal of the Atmospheric Sciences*, Vol. 52, 818–837, American Meteorological Society, 1995.

17. Evans, K. F. and G. L. Stephens, "Microwave radiative transfer through clouds composed of realistically shaped ice crystals. Part I: Single scattering properties," *J. Atmos. Sci.*, Vol. 52, 4367–4385, 1995.

18. Aydin, K. and C. Tang, "Millimeter wave radar scattering from model ice crystal distributions," *IEEE Transactions on Geoscience and Remote Sensing*, Vol. 35, No. 1, 140–146, 1997.